International Journal of Multiphase Flow 85 (2016) 173–176

Contents lists available at ScienceDirect

International Journal of Multiphase Flow

journal homepage: www.elsevier.com/locate/ijmultiphaseflow

Dual-luminescence imaging for capturing time-resolved temperature distributions of two-phase flow

H. Sakaue[a,*], K. Morita[b], S. Kimura[c]

[a] Department of Aerospace and Mechanical Engineering, University of Notre Dame, Notre Dame, IN 46556, USA
[b] Aeronautical Technology Directorate, Japan Aerospace Exploration Agency, Jindaijihigashi, Tokyo 182-8522, Japan
[c] Department of Mechanical Engineering, Kanagawa Institute of Technology, Atsugi, Kanagawa 243-0292, Japan

ARTICLE INFO

Article history:
Received 10 March 2016
Revised 1 June 2016
Accepted 7 June 2016
Available online 21 June 2016

Keywords:
Two-phase flow
Temperature
Time-resolved measurement
Luminescent Imaging

ABSTRACT

A dual-luminescence imaging method introduced in this paper captures time-resolved temperature distributions with unsteady flow structures for understanding two-phase flow phenomena. The method is featured as a time-resolved and non-intrusive measurement with high spatial and time resolutions. The spatial and time resolutions are mainly limited by the signal level from an optical setup of an imaging device. The absolute spatial and time resolutions can be limited by the size of the probe molecule and the thermal quenching process. The former is on the order of sub-nanometers and the latter is on the order of 10^{-12} to 10^{-8} s, respectively. The imaging system consists of two luminescent probes, color high-speed camera, and an illumination source. The illumination source can be a point, sheet, or volume illumination to locate the temperature measurement region of interest. The luminescent images from the two luminescent probes are simultaneously acquired by a color high-speed camera. By a ratio of the two-color images at each measurement-time frame, time-resolved temperature-dependent images can be captured. Time-resolved temperature distributions of supercooled-water droplet are shown as a demonstration of the dual-luminescent imaging method. A supercooled condition release is time-resolved with 1000 Hz image frame.

1. Introduction

Two-phase flow is complicated phenomenon due to the existence of moving and deformable interface and its interactions with the two phases (Ishii and Hibiki, 2005; Wallis, 1980; Cheng and Mewes, 2006). In the view of practical importance in advanced heat transfer systems, great efforts have been paid in this field. To understand this unsteady phenomenon by an experimental approach, a pressure drop measurement between the upper and lower sections of two-phase flow has been widely used (Mishima and Hibiki, 1996; Fourar and Bories, 1995; Xin et al., 1997; Tran et al., 2000; Lips and Meyer, 2011; Mansour et al., 2015; Zhai et al., 2015). However, this approach is not able to understand the local flow structures, because the pressure drop is a point measurement between the flow sections. By using a high-speed camera, time-resolved flow structures can be captured (Liu et al., 2015). However, this approach is limited to give qualitative flow structures. Numerical simulation is a great approach to describe two-phase flows to simulate flow structures as well as interfacial quantities (Ishii and Hibiki, 2005; Tryggvason et al., 2001). However, it is still challenging to obtain a time-resolved unsteady motion because of the computational time, and to enhance the simulation model, experimental approach is still necessary. In this paper, we introduce a dual-luminescence imaging method to capture the time-resolved two-phase flows. This gives time-resolved two-phase flow structures with a temperature as a quantitative value to understand the phenomenon. In this paper, we focus on a liquid-solid flow of supercooled water as a demonstration of the imaging method.

2. Method and system development

The dual-luminescence imaging system consists of dual luminescent water, a color high-speed camera, and an illumination source. It uses a luminescent method; the luminescent output can be related to the temperature distribution. By using the dual-luminescent water and illumination source, we can capture the luminescent output as a point/surface/volume of a target. Unlike an infra-red camera (IR camera), it does not contain the temperature information from the surroundings. By using a color high-speed camera, this method can capture the time-resolved temperature distribution of the target. Because a luminescent probe is a molecule, its size is less than a nanometer; the absolute

* Corresponding author.
E-mail address: hsakaue@nd.edu (H. Sakaue).

http://dx.doi.org/10.1016/j.ijmultiphaseflow.2016.06.002
0301-9322/

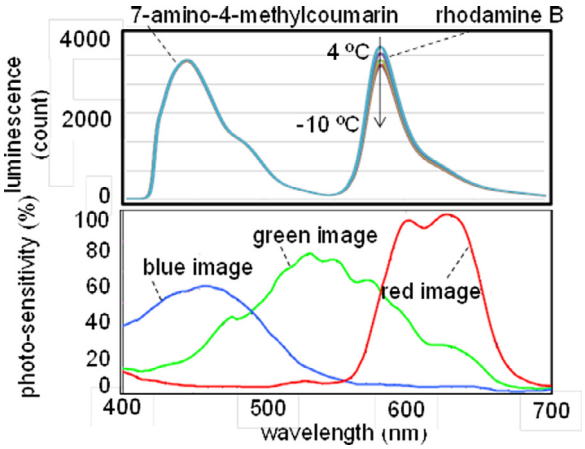

Fig. 1. Temperature spectra of the luminescent water consisting of 7-amino-4-methylcoumarin and rhodamine-B, and the photo-sensitivity of the high-speed color camera used (Phantom V710, Vision Research). (For interpretation of the references to color in this figure, the reader is referred to the web version of this article.)

limitation of the spatial resolution can be a nano scale or smaller. The probe changes its luminescent output by thermal quenching, which occurs on the order of 10^{-12} to 10^{-8} s (Lakowicz, 2006). This is the absolute time resolution of the dual-luminescence imaging method. Based on the spatial and time resolutions, this imaging method can be applied to a microscopic environment as well as larger facilities, such as industrial wind tunnels.

The luminescent water contains two luminescent molecules: rhodamine-B from Sigma-Aldrich and 7-amino-4-methylcoumarin from Tokyo Chemical Industry. The former is sensitive to the temperature, and the latter is insensitive to the temperature. These are dissolved in water with very small amount to keep the physical properties of water. The concentrations of these luminophores were 10 μM and 1 μM, respectively. A high-speed color camera (Phantom V710, Vision Research) was used to acquire the time-resolved luminescent outputs from these luminescent molecules. The camera has a Bayer filtered on an image chip to separate the luminescent outputs as red-, green-, and blue-images. Fig. 1 shows the temperature spectra of the luminescent water and the photo-sensitivity of the camera. We can see that two luminescent peaks exist at 440 and 580 nm. The peak at a lower wavelength, which was obtained from 7-amino-4-methylcoumarin, was temperature insensitive. On the other hand, the peak at a higher wavelength, which was obtained from rhodamine-B, was temperature sensitive due to thermal quenching (Liu and Sullivan, 2004). Both peaks were matched with the blue- and red-images of the camera.

Consider the luminescent outputs from an arbitrary pixel ij at an arbitrary time t on an image chip of the color camera, where the image chip has m by n pixels ($i=1, 2, \ldots, m$, and $j=1, 2, \ldots, n$). At pixel ij, the outputs from the blue image, $V_{Bij,t}$, and the red image, $V_{Rij,t}$, can be described as:

$$V_{Bij,t} = G_{ij,t}\cdot\left(I_{CRij,t} + \Delta I_{CRshot}\right) + N_{ij}, \tag{1}$$

$$V_{Rij,t} = G_{ij,t}\cdot\left(I_{RMij,t,T} + \Delta I_{RMshot}\right) + N_{ij}, \tag{2}$$

where I_{CR} and I_{RM} are the luminescent intensities from 7-amino-4-methylcoumarin and rhodamine-B, respectively. ΔI_{CRshot} and ΔI_{RMshot} are the shot noise associated with I_{CR} and I_{RM}, respectively. Because rhodamine-B was temperature sensitive, I_{RM} is temperature dependent. It is indicated by the subscript T in Eq. (2). N indicates the camera dark noise at the pixel ij. This noise factor can be obtained by blocking the luminescent input to the camera. Here, $G_{ij,t}$ is the geometric factor varied by the pixel location. It is related to the shape and location of a droplet in an image frame, non-uniformity of the illumination source, and the distance of the droplet and camera. Because the shape and location of a water droplet can be changed during the measurement, three factors above can be time dependent. To cancel $G_{ij,t}$ from the luminescent image, a luminescent ratio shown in Eq. (3) was derived (Sakaue et al., 2013).

$$\begin{aligned} S_{ij,t} &= \left(V_{Rij,t} - N_{ij}\right)/\left(V_{Bij,t} - N_{ij}\right) \\ &= \left(I_{RMij,t,T} + \Delta I_{RMshot}\right)/\left(I_{CRij,t} + \Delta I_{CRshot}\right), \end{aligned} \tag{3}$$

Eq. (3) cancels the geometric factor, $G_{ij,t}$. When signal-to-noise ratio (SNR) is high enough, such as

$$I_{CRij,t}, I_{RMij,t,T} >> \Delta I_{CRshot}, \Delta I_{RMshot}, \tag{4}$$

Eq. (3) can be rewritten as

$$S_{ij,t} \approx I_{RMij,t,T}/I_{CRij,t}, \tag{5}$$

As an image, S can be related to a temperature distribution at an arbitrary time, t. It can be obtained by rationing the red and blue images after subtracting the dark noise. At a pixel where I_{RM} and I_{CR} are zero or low signal, the ratio of the two showing Eq. (3) would give plus or minus infinity. To avoid this processing error, a threshold can be assigned to each pixel location. For instance, if $I_{RMij,t}$ or $I_{CRij,t}$ is lower than the mean shot noise or saturated signal, the ratio, $S_{ij,t}$, is assigned to be zero.

2.1. Temperature calibration result

The luminescent ratio, S, can be converted to the temperature map through a temperature calibration. A droplet of the luminescent water with 4-mm in diameter was placed on a temperature-controlled plate. The plate as well as the surrounding air was cooled from −12 to 4 °C in a temperature-controlled room (PWU-3KP, ESPEC). The temperature of the droplet was directly measured by a thermocouple (K-316, Toyonetsu Kagaku). Here, the droplet as well as the surrounding was the same temperature and the droplet was at stationary during the calibration. Thus the size of a thermocouple did not influence to the temperature measurement. It was not a colliding surface to create ice. The temperature calibration was repeated five times to obtain the mean and standard deviation as an error. The peak ratio of the two luminescent outputs may be different from cameras and luminescent water used. To normalize the peak ratio, Eq. (5) was normalized at the reference condition.

$$S_{calib} = \alpha\cdot I_{RM,T}/I_{CR}, \tag{6}$$

$$\alpha = I_{CR,Tref}/I_{RM,Tref}, \tag{7}$$

where, α can be determined by the two luminescent outputs at the reference temperature, T_{ref}, which was 0 °C for this calibration. Fig. 2 shows the temperature calibration of the ratio, S_{calib}. A relatively large error can be seen at lower temperatures. This is due to the uncertainty of the temperature-controlled room to provide a low temperature inside the room. As described in Eq. (8), S_{calib} is a function of the temperature. The first order polynomial was fitted to the calibration results.

$$S_{calib} = c_{T0} + c_{T1}\,T, \tag{8}$$

where c_{T0} and c_{T1} are calibration coefficients which can be determined experimentally. The slope of the calibration at the reference temperature was defined as the temperature sensitivity, σ_T (%/°C).

$$\sigma_T = c_{T1}, \tag{9}$$

The temperature sensitivity, σ_T, was −1.6 (%/°C). By a selection of luminescent probes and a color camera, σ_T is determined, because of the changes in luminescent spectrum, temperature sensitivity of the probes, and camera photo-sensitivity.

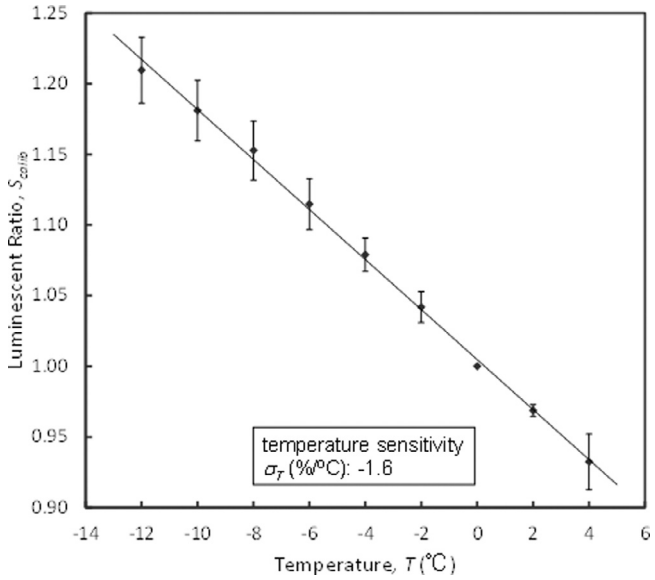

Fig. 2. Temperature calibration results.

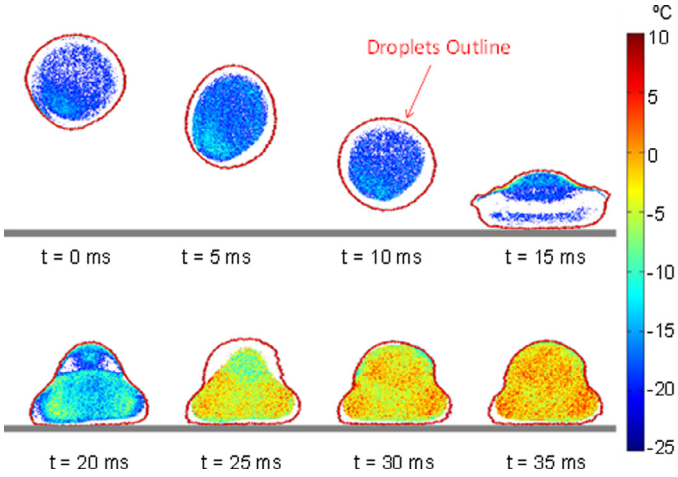

Fig. 3. Time-resolved temperature distributions of a supercooled-water droplet colliding on a surface.

The time-resolved temperature information at each pixel location, T_{ij}, can be obtained from an image ratio, α, and calibration coefficients. The latter two factors are determined by the temperature calibration.

$$T_{ij} = [\alpha/(c_{T0} + c_{T1})] \cdot \left(V_{Rij,t} - N_{ij}\right)/\left(V_{Bij,t} - N_{ij}\right), \tag{10}$$

Eq. (10) was obtained by combining, (7), and (8).

3. Demonstration of dual-luminescence imaging method

A collisional icing by a supercooled-water droplet is caused by a small water droplet with its size on the order of micrometers to millimeters (Jeck, 2002; Lewis et al., 1947; Cober et al., 2001). To give the time-resolved temperature map of the icing process, spatial resolution should be smaller than the droplet diameter. The time resolution is required to be on the order of milliseconds or faster to resolve the icing process. However, a conventional technique, such as a thermocouple, is not appropriate to measure the temperature, because the thermocouple surface itself becomes a collisional surface. A conventional thermocouple is relatively large to resolve the distribution of a single droplet with its size on the order of millimeters or smaller. An IR camera has been used as a non-intrusive method to detect the temperature information (Meola and Carlomagno, 2004). This method relates the IR output from a detecting object to the temperature. It only requires an IR camera that is a simple and non-intrusive method. Even though its simplicity, a mirror-finish surface tends to reflect a surrounding temperature that needs to be corrected. Because of measuring IR signal, it gives lower signal at a lower temperature, which changes on the order of the fourth power by Stefan–Boltzman law. This method captures the temperature distributions of the detecting object with surroundings as a whole image; the temperature information at a desired area, for example inside of the object, is not possible.

3.1. Time-resolved temperature measurement result

The time-resolved temperature distributions of a supercooled-water droplet were captured by the dual-luminescence imaging (Fig. 3). The luminescent images were acquired at the camera frame rate of 1000 Hz. Representative temperature maps were shown every 5 ms. A threshold was set to remove uncertainty caused by low SNR and saturated outputs. The temperature at the threshold regions was not obtained. The outline of the droplet shape was overlaid to each temperature measurement. This was obtained from a raw image at each time frame. A threshold of S_{calib} was set between 0.90 and 1.25 to remove uncertainty caused by low SNR image. A luminescent water droplet with 2-mm in diameter was released 10 mm from the plate surface. It contains 7-amino-4-methylcoumarin and rhodamine-B with the same concentration used for the temperature calibration. Based on the freezing test under atmospheric conditions, pure water and the luminescent water were both frozen at 0 °C. The plate as well as the surrounding was kept at −15 °C inside the temperature-controlled room. The droplet was a pseudo-spherical shape during the dropping. The temperature of the droplet was −15 °C. We can see that the droplet changed its shape during the collision on the plate surface. At $t = 15$ ms, a higher temperature at the upper part of the droplet will be an initiation of supercooled condition. This was propagated to the lower part of the droplet at $t = 20$ ms. Between 20 and 25 ms, the supercooled condition began to be released, which can be seen by the temperature distribution. At 35 ms, the supercooled condition was released almost for the entire droplet. We can see a dominant temperature from the temperature map at 0 °C.

After the supercooled condition release, the droplet will be completely iced. This involves the recrystallization. The luminescent intensity will be increased by the recrystallization due to an increase of the concentration of the luminescent water. However, the intensity change by the concentration can be cancelled by taking a ratio, which is described in Eqs. (1) to (3). If the luminescent molecules exist in water, the luminescent intensity can be observed. However, when the liquid phase completely changed to the ice phase, the luminescent molecules will be squeezed out from ice by recrystallization. At this phase, the luminescent molecules are no longer present in ice so that the luminescent intensity will not be observed in ice.

4. Conclusion and summary

We presented a dual-luminescence imaging method that can capture the time-resolved temperature distributions with flow structures of a two-phase flow. Temperature-sensitive and temperature-insensitive luminescent probes (rhodamine-B and 7-amino-4-methylcoumarin) were used to give the luminescent outputs acquired by a high-speed color camera. By rationing the two luminescent images, the time-resolved temperature distributions

of a supercooled-water droplet colliding on a surface were obtained. In the present letter, the imaging method was applied to a two-phase flow with a target size on the order of millimeters. A sheet illumination can be selected to give the time-resolved 2-D profiles of the temperature distributions of a target object. The method can be applied to smaller or larger scale. The absolute spatial resolution can be as small as the size of the luminescent probes, which is on the order of sub-nanometers. The larger scale does not have an obvious limitation, which can be limited by the optical setup. The absolute time resolution is the thermal quenching process of the probes, which is on the order of 10^{-12} to 10^{-8} s. Even though its absolute limitations, the limitation of the imaging capability will occur by the camera frame rate associated with the luminescent signal level. The presented imaging method can be used to a liquid-gas phase flow, such as a boiling process of water.

Acknowledgment

The present study was supported by JAXA Grants in Exploratory Research. Authors would like to acknowledge Mr. Mio Tanaka at JAXA as a degree-seeking student for his technical assistance.

References

Cober, S.G., Isaac, G.A., Strapp, J.W., 2001. J. Appl. Meteorol. 40, 1984–2002.
Cheng, L., Mewes, D., 2006. Int. J. Multiph. Flow 32, 183–207.
Fourar, M., Bories, S., 1995. Int. J. Multiph. Flow 21 (4), 621–637.
Ishii, M., Hibiki, T., 2005. Thermo-fluid Dynamics of Two-Phase Flow. Springer Verlag, Heidelberg, Germany.
R.K. Jeck, Federal Aviation Administration, DOT/FAA/AR-00/30 (2002).
W. Lewis, D.B. Kline, C.P. Steinmetz, National Advisory Committee for Aeronautics Technical Note no. 1424 (1947).
Lips, S., Meyer, J.P., 2011. Int. J. Multiph. Flow 37, 845–859.
Liu, X.F., Xia, G.D., Yang, G., 2015. Int. J. Multiph. Flow 73, 227–237.
Lakowicz, J.R., 2006. Principles of Fluorescence Spectroscopy. Springer Verlag, Heidelberg, Germany, p. 5.
Liu, T., Sullivan, J.P., 2004. Pressure and Temperature Sensitive Paints (Experimental Fluid Mechanics). Springer Verlag, Heidelberg, Germany, pp. 8–10.
Meola, C., Carlomagno, G.M., 2004. Meas. Sci. Technol. 15, R27–R58.
Mishima, K., Hibiki, T., 1996. Int. J. Multiph. Flow 22 (4), 703–712.
Mansour, M.H., Kawahara, A., Sadatomi, M., 2015. Int. J. Multiph. Flow 72, 263–274.
Sakaue, H., Miyamoto, K., Miyazaki, T., 2013. J. Appl. Phys. 113 (8), 084901-084901-8.
Tran, T.N., Chyu, M.-C., Wambsganss, M.W., France, D.M., 2000. Int. J. Multiph. Flow 26, 1739–1754.
Tryggvason, G., Bunner, B., Esmaeeli, A., Juric, D., Al-Rawahi, N., Tauber, W., Han, J., Nas, S., Jan, Y.-J., 2001. J. Comput. Phys. 169, 708–759.
Wallis, G.B., 1980. Int. J. Multiph. Flow 6 (1), 97–112.
Xin, R.C., Awwad, A., Dong, Z.F., Ebadian, M.A., 1997. Int. J. Heat Fluid Flow 18, 482–488.
Zhai, L.-S., Jin, N.-D., Zong, Y.-B., Hao, Q.-Y., Gao, Z.-K., 2015. Int. J. Multiph. Flow 76, 168–186.